Clinical Plasma Medicine 19–20 (2020) 100103

Contents lists available at ScienceDirect

Clinical Plasma Medicine

journal homepage: www.elsevier.com/locate/cpme

Breast cancer treatment using cold atmospheric plasma generated by the FE-DBD scheme

Ban H. Adil[a], Ahmed Majeed Al-Shammari[b,*], Hamid H. Murbat[a]

[a] University of Baghdad, College of Science for Women, Baghdad, Iraq
[b] University of Al-Mustansiriyah, Iraqi Center for Genetics and Cancer Research, Baghdad, Iraq

ARTICLE INFO

Keywords:
Cold atmospheric plasma
FE-DBD
Breast cancer therapy
Growth inhibition
ROS

ABSTRACT

Background: Cold atmospheric plasma (CAP) is widely used in the cancer therapy field. This type of plasma is very close to room temperature. This paper illustrates the effects of CAP on breast cancer tissues both in vivo and in vitro.

Methods: The mouse mammary adenocarcinoma cell line AN3 was used for the in vivo study, and the MCF7, AMJ13, AMN3, and HBL cell lines were used for the in vitro study. A floating electrode-dielectric barrier discharge (FE-DBD) system was used. The cold plasma produced by the device was tested against breast cancer cells.

Results: The induced cytotoxicity percentages were 61.7%, 68% and 58.07% for the MCF7, AMN3, and AMJ13 cell lines, respectively, whereas the normal breast tissue HBL cell line exhibited very little or no cytotoxicity. Reactive oxygen species (ROS) were measured, and we found that more ROS were generated under the impact of CAP in cancer cells, whereas the normal HBL cell line had the lowest ROS level. The in vivo study showed that CAP treatment could reduce the volume of treated tumors compared to those in untreated mice.

Conclusions: CAP has anticancer effects both in vitro and in vivo and this effect is mediated by the ROS and induce apoptosis in p53 independent pathway. the current method is promising for breast cancer therapy.

1. Introduction

Plasma is the fourth state of matter and is represented by a quasi-neutral gas consisting of neutral and charged particles that demonstrate collective behavior. Plasma forms approximately 99% of universal matter as electrified gases of dissociated positive ions and negative electrons of atoms; thus, atmospheres, interstellar hydrogen, gaseous nebulae, and stellar interiors are types of plasma [1]. Plasma is a gassy mixture of electrons and positive or negative ions that can be partially ionized, such as the plasma generated in fluorescent lamps, or fully ionized, such as the plasma generated in the sun [2]. There are two types of plasma (thermal and nonthermal), which are based on the temperature of the electrons with respect to that of the other particles (ions and neutral particles). In thermal plasma, the electrons and heavy particles are in thermal equilibrium (have nearly the same temperature), whereas in nonthermal plasma, the heavy particles are nearly at room temperature and the electrons have a much higher temperature. Conventional thermal plasma temperatures are greater than 3000°C at the target, making plasma a typical application for mineralogy but unsuitable [3] for treatment of living tissue. Nonthermal plasma is also called cold plasma; at the point of application, cold plasma has a temperature of less than 40°C, which makes it suitable for treatment of living tissue [4–6]. Cold plasma can be generated at low and high pressure (atmospheric pressure). Various types of CAP systems are used as plasma-based cancer therapy; these systems depend on electrical discharge, such as corona discharge systems, dielectric barrier discharge (DBD), micro hollow cathode discharge (MHCD), and atmospheric pressure plasma jet (APPJ) systems. Each of these systems has unique properties, characteristics, and applications [7]. A special type of DBD system is the floating electrode dielectric barrier discharge (FE-DBD) system. The difference between the DBD and FE-DBD systems is that the second electrode of the DBD is grounded, whereas the electrode in the FE-DBD is not grounded and instead is represented by a sample, tissue, or organ; the powered electrode must be close to the surface of the second electrode to achieve discharge and thus generate cold atmospheric plasma [8]. The most important use for cold plasma in medicine is wound healing, sterilization, and cancer therapy, which is the focus of this study. The ability of non-thermal plasma to treat various types of cancers effectively by selectively killing cancer cells while leaving normal tissue unharmed has been tested [9,10].

* Corresponding author: Department of Experimental Therapy, Iraqi Center for Cancer and Medical Genetic Research, Al-Mustansiriyah University.
E-mail address: ahmed.alshammari@iccmgr.org (A.M. Al-Shammari).

https://doi.org/10.1016/j.cpme.2020.100103
Received 11 October 2019; Received in revised form 22 May 2020; Accepted 26 May 2020

Experiments identified a plasma dose that caused minimal immediate toxicity and stimulated apoptosis in a cancer cell line [8]. Breast cancer is fifth leading cause of death from cancer and number one in women worldwide [11] Breast cancer occasionally is associated with generation of mutations but usually is a genetic disease of somatic cells. Breast cancer can be considered a metastatic tumor that commonly is located at the axillary nodes, but remote metastasis can occur to sites containing bone or bone marrow [12]. Breast cancer frequently develops drug resistance during chemotherapy, which lead to impaired treatment of breast cancer and increase mortality [13]. Therefore, there is need to overcome this resistance by means of novel therapeutics such as CAP. The aim of the current research is to study the effect of CAP as a breast cancer therapy using both in vitro and in vivo models with a locally constructed FE-DBD system.

2. Materials and Methods

2.1. Floating electrode dielectric barrier discharge (FE-DBD)

The constructed FE-DBD system which described earlier [14] consists of two essential parts: *probes and a high voltage source.* Two types of probes were constructed according to the applications of the system (*in vivo* or *in vitro*):

1- probes with small diameters ranging between 2 and 5 mm (used for the in vitro study) and
2- probes with large diameters ranging between 10 and 20 mm (used for the *in vivo* experiments).

2.1.1. Small probes

This type of probe consists of two basic parts. (i) *The base of the probe:* a small plastic bottle with a length of 10 cm and a diameter of 4 cm with a changeable cap that is used as a base for the external probe (Fig. 1). An isolated metal wire passes through the bottle and connects from its ends with a spring. The other side of this spring is connected to a piece of conductive metal that penetrates a circular insulator barrier (Fig. 1) with a diameter equal to the inner diameter of the bottle nozzle. Both of the spring and the insulator barrier are fixed in the bottle nozzle such that conductive metal is directed outside the bottle to represent the high-voltage electrode (Fig. 1). (ii) *The external probe:* this probe consists of a metal rod (stainless steel) covered by an insulator (Pyrex glass) with a thickness of 1 mm except for a distance of 1 mm on the left stripper without a cover, as shown in Fig. 1. The probe is fixed on the center of the bottle stopper from outside; thus, the probe is directed outwards and passes through the stopper to contact a metal piece fixed in the inner stopper. When the stopper is tightened to the bottle, the metal tip fixed on the bottle is touched to a metal piece (Fig. 1). When the other side of the wire is connected to the high-voltage terminal of the high-voltage source, the electrical circuit is completed."

The poles were designed with various diameters ranging from 2-5 mm, as shown in Fig. 1. When the high voltage source is powered and the probe approaches living tissue to a distance of 3 mm or less, plasma is generated between the probe and tissue.

2.1.2. Large probes

This probe is composed of a copper rod with a length of 150 mm and diameter of 2 mm. The rod ends in a float base with a diameter of 20 mm. The rod and base are covered by fiberglass with a thickness of 24 mm except for a distance of 2 mm at the end of rod left stripper without a cover; thus, the fiberglass has cylindrical shape and the rod passes through its center, whereas the face of the base is covered by Pyrex glass with a thickness of 1 mm, as shown in Fig. 2. The end of the rod is connected by wire to the high-voltage terminal of the high-voltage source. When the high-voltage source is powered and the probe approaches living tissue to a distance of 3 mm or less, plasma is generated between the probe and tissue.

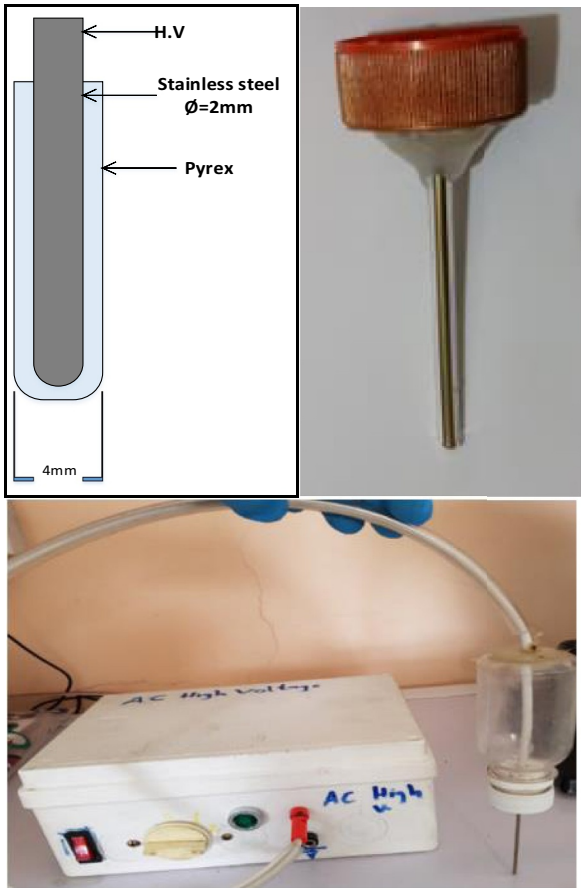

Fig. 1. Small Probe of the Proposed FE-DBD. the polymer that constitutes the "plastic bottle" that used as base of the probe was Polyethylene terephthalate.

2.1.3. High-voltage source

The HV source was designed especially for the proposed system. The high-voltage source circuit is shown in Fig. 3. The circuit was based on a special type of transformer called a flyback transformer (FBT). This type of transformer can raise the voltage to several thousand volts

The circuits are fed by a continuous voltage equal to 12 V. This circuit depends on an integrated circuit (IC) called a Timer555 and is represented by an oscillator. The oscillation time changes from a few to thousands of pulses per second. The output voltage is variable up to 25 kV, and its frequency varies up to 30 kHz to provide variable voltage (0-25) kV and variable frequency (0-30) kHz, as shown in Fig. 3. The given system can be characterized to various voltage, thus frequency, current and power. In the experimental attempts, when the voltage is 13.2, 23.67, 33.44 (V), the frequency is 70, 73.9, 76.8 (kHz), the current is 0.5, 0.7, 1.7 (mA), and the power is 6.6, 16.6, 56.84 (W), respectively. In the current work the applied voltage was 13.2KV and the frequency was 70kHz.

2.1.4. Cell culture

The human breast cancer AMJ13 and the mouse mammary adenocarcinoma AMN3 cell lines, were cultured in a RPMI-1640 medium with 10% fetal bovine serum (FBS), 100 units/mL penicillin, and 100 µg/mL streptomycin. The human breast cancer MCF7 cell line and HBL normal epithelial breast tissue cell line were cultured in MEM medium with 10% fetal bovine serum (FBS), 100 units/mL penicillin, and 100 µg/mL streptomycin. These cell lines were provided Mustansiriyah University, Iraqi Center for Cancer and Medical Genetic Research (ICCMGR), Experimental Therapy Department, Cell Bank Unit. These cells incubated at 37°C with 5% CO2.

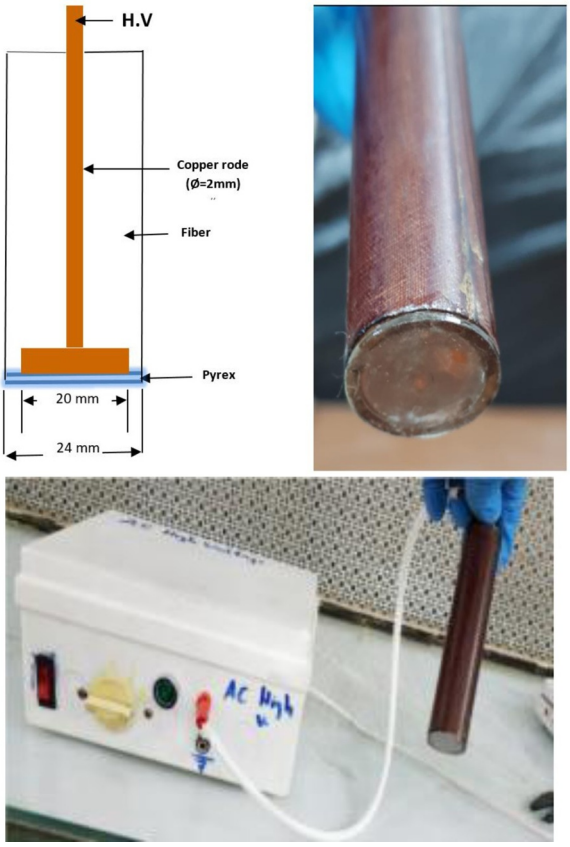

Fig. 2. Large Probe of the Proposed FE-DBD.

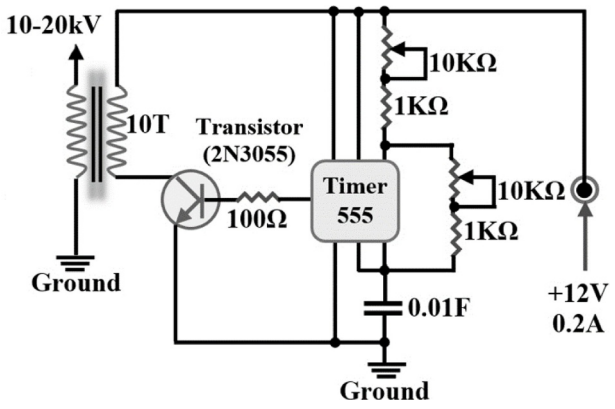

Fig. 3. Electrical Circuit Used as the High-Voltage Source.

2.2. In Vitro Study

Our study used four types of cancer cell lines: human breast cancer MCF7 and AMJ13 cells and mouse mammary adenocarcinoma AMN3 cells as breast cancer cell lines and HBL cells as a normal epithelial breast tissue cell line. A 96-well (12 × 8) microplate was used for tissue culture. Each well was seeded with 10,000 cancer cells in 100µl media and incubated at 37°C for 24 hours until a confluent monolayer was observed under an inverted microscope. The cells were exposed to CAP using the proposed plasma generator system with a small diameter probe Fig. 4 for three different intervals (5, 10, and 15 sec); the control wells received no treatment. The described steps were performed in triplicate, and the plates were incubated again at 37°C for different intervals (24, 48, and 72 hrs). After incubation, the growth medium was decanted. The following steps were repeated three times to confirm the veracity of the results:

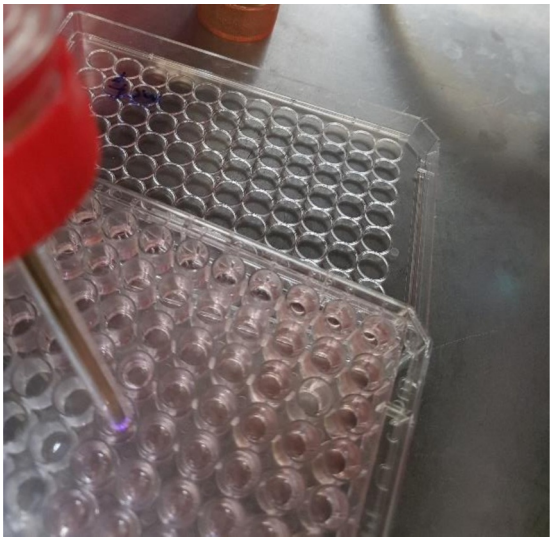

Fig. 4. Exposure of the tissue culture to CAP

a MTT assay (100 µL of MTT diluted with 1 mL of serum-free medium) was added to the cells (100 µL of diluted MTT per well) and incubated for 2 hours. Then, the medium was decanted, and dimethyl sulfoxide (DMSO) was added (50 µL per well). The plate was incubated for 40 min at 37°C; during this step, the percentage of live cells will be determined according to the darkness of the violet color in the resulting solution. Therefore, the solution from the control group has the darkest violet color.

b Crystal violet assay (100 µL/well) was added, and the cells are incubated for 20 min at 37°C. A microplate reader was used to read the results at the 580 nm wavelength and to evaluate the percentage of live cancer cells (inhibition rate). The mean value was computed for each group [15].

The computed mean inhibition percentages at 24, 48, and 72 hours were recorded separately for the results analysis.

2.2.1. Reactive oxygen species (ROS) measurement assay

For this study, the Abcam® DCFDA Cellular ROS Detection Assay Kit (ab113851; Abcam, UK) was used to assess the ROS produced in response to the CAP treatment. Cells were harvested and seeded into 96-well microplates in the dark at a density of 10,000 cells per well. Serum-free medium (SFM) was added (100 µL/well), and the plates were incubated for 24 hours at 37°C. The SFM was decanted, and the cells were washed with 100 µL/well of 1X buffer. Immediately, the 1X buffer was decanted, and 100 µL/well of diluted DCFDA assay solution was added. The cells were incubated for 45 min at 37°C in the dark. The DCFDA assay solution was removed, and 100 µL/well of supplement buffer was added. The wells were exposed to CAP for different durations (5, 10, and 15 sec) and then incubated for 3 hours at 37°C.

The microplates were measured using a fluorescence reader (Ex/Em = 485/535 nm).

Fluorescence microplate measurement: Blank readings must be subtracted from all measurements to assess the fold change from the assay control.

2.2.2. Gene expression analysis

Gene expression was analyzed for the treated cells using primers supplied by Integrated DNA Technologies (USA) to evaluate the effect of the proposed CAP system on selected genes P53, caspase-8 and 9 and GAPDH as housekeeping gene (Table 1).

The Magnesia® Total RNA Cultured Cell Kit (AE6101-AE6102) was used for total RNA purification from up to 10^6 cultured cells (Anatolia Geneworks, Turkey) [16], and the KAPA^{TM} SYBR® Fast One-Step qRT-

Table 1
Primers Used for the gene expression study

#	Primer	H/M	F/R	Sequence '5 - … -'3
1	P53 [19]	Human	Forward	CCGTCCCAAGCAATGGATG
			Reverse	GAAGATGACAGGGGCCAGGAG
		Mice	Forward	GATCTGTTGCTGCCCCAGGAT
			Reverse	AGATGACAGGGGCCATGGAGT
2	CASP8 (Caspase8)	Human	Forward	GACCACGACCTTTGAAGAGCTTC
			Reverse	CAG CCT CAT CCG GGA TAT ATC
		Mice	Forward	GCTCTGAGTAAGACCTTTAAGG
			Reverse	GATCTTGGGTTTCCCAGAC
3	CASP9 (Caspase9)	Human	Forward	CTC TTG AGC AGT GGC TGG TC
			Reverse	GCTGATCTATGAGCGATACT
		Mice	Forward	GCTGTTTCTGCGAAAGGGACT
			Reverse	AGGGCACAATCCCTAACCAC
4	GAPD [20]	Human	Forward	ATCACTGCCACCAGAAGACTG
			Reverse	AGGTTTTTCTAGACGGCAGGTCAG
		Mice	Forward	TGGCCGTATTGGGCGCCT
			Reverse	TCTCCATGGTGGTGAAGA

PCR Kit (KK4651) was used for real-time PCR with RNA as a template (KAPA Biosystems, USA). All of the necessary buffers are provided with the kits [17].

RNA was extracted from MCF7 (human), AMJ13 (human), and AMN3 (mice) cells that were seeded in two 12-well (4 × 3) microplates (5×10^4 cells/well) and then incubated for 24 hours at 37°C. After incubation, the cells were exposed to CAP for 10 sec; an unexposed group was considered the control. One microplate was re-incubated for 24 hours, and the other was re-incubated for 48 hours. After re-incubation, the cells were lysed, and 0.5 mL of PBS was added per well. The cells and the added PBS were removed to a 1.5 mL Eppendorf tube. The Eppendorf tube was centrifuged to precipitate the cells for 5 min at 110 rpm, and then the PBS was decanted. β-ME was mixed with RB buffer (10 µL of β-ME was added to 1 mL of RB buffer in a tube). A total of 200 µL of the resulting solution was added per Eppendorf tube and placed in the Magnesia Automated DNA/RNA Extraction Device to extract the RNA.

The concentration and purity of the extracted RNA were measured by a spectrophotometer; the concentration is measured in ng/µL unit, and the purity is measured as the optical density (OD) ratio at 260/280 nm (the DNA and protein absorption wavelengths). The accepted purity of the RNA is 1.7-1.9 [12]. The RNA concentration in the samples was normalized according to the lowest concentration in the samples using the following Eq. (1):

$$V_n = \frac{C_0 \times V_0}{C_n} \tag{1}$$

where C_0 is the lowest concentration, V_0 is the normalization volume (equal to 100 µL), C_n is the current sample concentration, and V_n is the volume of the current sample that will be diluted by triple distilled water (tdH_2O) to generate a 100 µL volume. To prepare the primer solutions, the primers were dissolved in tdH_2O to a unified concentration of 100 µM/µL, which was called the stock solution. A total of 50 µL of the stock solution was added to 150 µL of tdH_2O to obtain a solution with a concentration of 25 µM/µL for use in the PCR (polymerase chain reaction). The qPCR was performed in a 20 µL reaction solution by mixing the following materials:

1 1.5 µL of the forward (F) primer, (concentration: 25 µM/µL);
2 1.5 µL of the reverse (R) primer (concentration: 25 µM/µL);
3 10 µL of qPCR Master Mix Buffer (2X) (concentration: 1X);
4 0.5 µL of RT Mix Buffer (50X) (concentration: 1X); and
5 6.5 µL of the extracted RNA template.

The generated solution was placed in a real-time PCR machine for the thermal reaction to measure the cycle threshold (CT) value. The cycling protocol was described in Table 2:

Table 2
PCR Cycling Protocol

#	Step	Temperature			Duration			Cycles
1	cDNA Synthesis	42°C			5 min			Hold
2	Inactivate RT	95°C			2-5 min			Hold
3	Denature	95°C			3 sec			40
4	Anneal	57°C			≥ 20 sec			40
5	Extension	95°C	55°C	95°C	1 min	1 min	1 min	-
6	Dissociation	72°C			20 sec			-

PCR is used to quantify gene expression levels. The measured CT values during the thermal reaction were recorded to compute the $2^{-\Delta\Delta CT}$ measurement. This method assumes that the PCR amplification efficiency is equal to 1 (i.e., 100%) under ideal conditions; therefore the value is 2 = 1 + amplification efficiency [18].

2.3. C. In Vivo Study

The in vivo study was approved by the scientific Committee of Baghdad University, College of Science for women. This study was conducted using female albino Swiss mice 6–8-week-old injected into the right flanks with AN3 mammary adenocarcinoma cells [21]. When the tumors nodules reached 0.5–1 cm in diameter, the mice bearing tumor were divided randomly in to four groups. One of these groups was considered a control group and did not receive any treatment. The other three groups were subjected to one of three cold atmospheric plasma (CAP) exposure durations (20, 40, and 50 sec). The tumor volume was measured as the height and width of the tumor. The mouse weights were also measured, and the mean volume and weight values for the three mice in each group were compared with those of the control group to estimate the effect of each plasma dose. The hair of the mice was removed to establish direct CAP treatment on the skin. CAP is generated when the floating electrode of the plasma system touches the mouse body (the other electrode) to represent the discharge concept Fig. 5. The mice were exposed to plasma three times during the first week with 48-hour intervals between exposures and kept under observation for 21 days to record the tumor response to therapy following CAP exposure. The tumor volume was calculated three times per week. The width and length of the tumor were measured using a Vernier caliper, and the tumor volume was assessed using the following Eq. (2):

$$V_T = \frac{w \times L^2}{2} \tag{2}$$

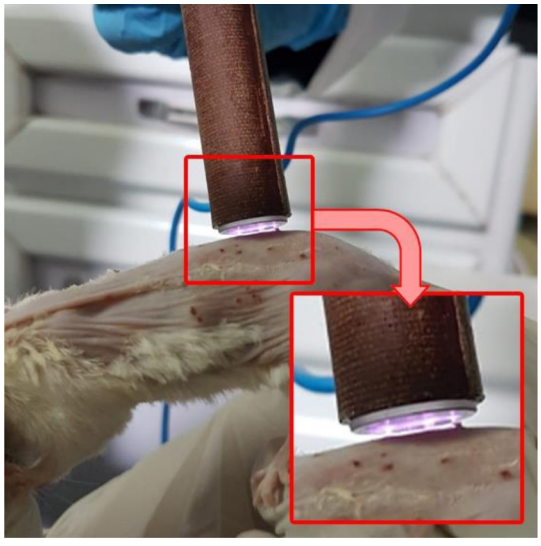

Fig. 5. CAP exposure method

where V_T is the tumor volume, w is the tumor width, and L is the tumor length. The relative tumor volume (RTV), cytotoxicity or tumor growth inhibition (GI) ratio, and relative mouse weight (RMW) were also calculated using the following equations:

$$V_R = \frac{V_T(d_i)}{V_T(d_0)} \tag{3}$$

$$GI_{\%} = \frac{V(control) - V(treated)}{V(control)} \times 100\% \tag{4}$$

$$W_R = \frac{W(d_i)}{W(d_0)} \tag{5}$$

where V_R and W_R represent RTV and RMW, respectively, d_i is the i^{th} day, d_0 is the day the treatment started, $GI_{\%}$ is the GI ratio, G_c and G_E are the control and exposed groups, respectively, and W is mouse weight measured using a sensitive balance.

3. Results

The experiments were performed at the Iraqi Center for Genetics and Cancer Research, Mustansiriyah University, and were analyzed using GraphPad Prism v7.0 to estimate the impact of the proposed CAP system on breast cancer tissues both *in vivo* and *in vitro*.

In the *in vitro* experiments, cytotoxicity was measured for three breast cancer cell lines (MCF7, AMJ13, and AMN3) under different CAP doses (5, 10, and 15 sec) compared with the impact of plasma on the HBL normal breast tissue cell line. In the MCF7 cells, the maximum cytotoxicity was 61.7%, which occurred with the 5-sec exposure followed by 48 hrs of incubation Fig. 6. In the AMJ13 cells, the maximum cytotoxicity was 68% following the 10-sec exposure and 72 hrs of incubation Fig. 7. The AMN3 cells showed maximum cytotoxicity of 58.07% after the 10-sec exposure and 48 hrs of incubation Fig. 8. Conversely, the HBL cells exhibited very little or no cytotoxicity Fig. 9.

3.1. Morphological study

The CAP-treated cells showed lower cell numbers due to detachment in all observed fields. Moreover, condensed nuclei were noted, indicating cell death. The images in figs. (6–9) show the 3x exposure. The control untreated breast cancer cells continued to grow to form overgrowth in the observed fields under an inverted microscope and were photographed using a digital camera.

3.2. Reactive oxygen species (ROS) measurement

Using the same cell lines, the intracellular ROS generated under the impact of CAP was measured. The cancer cell lines had the highest ROS level, whereas the HBL cell line had the lowest (both after the 15 sec exposure). Fig. 10 exhibits the exact ROS levels generated.

3.3. CAP effect on gene expression of treated cells

Finally, gene expression was evaluated for three different proteins using Ct values obtained from qRT-PCR analysis. P53, CASP8, and CASP9 were measured in the human breast cancer cell lines MCF7 and AMJ13 and the mouse breast cancer cell line AMN3. In the MCF7 cells, P53 and CASP8 were downregulated after both the 24 and 48 hr incubation durations, whereas CASP9 was upregulated at 24 hrs by 2.73-fold and by 3.82-fold at 48 hrs. In the AMJ13 cells, both P53 and CASP9 were downregulated at both 24 and 48 hrs of incubation, whereas CASP8 was upregulated by 2.79-fold at 24 hrs but downregulated by 0.83-fold at 48 hrs. P53 was still downregulated in the AMN3 cells at both 24 and 48 hrs of incubation. CASP8 and CASP9 were also downregulated at 24 hrs, but both genes were upregulated at 48 hrs by 1.96- and 1.06-fold, respectively. Fig. 11 a, b, c and Table 3 illustrate the upregulation and downregulation of the referenced genes in the cell lines.

3.4. In vivo tumor growth inhibition by CAP treatment

In the *in vivo* experiments, growth inhibition was calculated relative to the tumor volume of the control group using Eq. (3). The results showed at the end of the experiment (day 30) that 20 and 40 sec CAP exposure gave the maximum growth inhibition ratio of 96%, and 96% respectively, while 50 sec exposures gave ratios equal to 87%, as shown in Fig. 12. The RTV ratios were calculated using Eq. (4), which represented the tumor volumes on the i^{th} day relative to the tumor volume on day zero. The minimum ratio was found for the 20 sec exposure and was equal to 25%; the 40 and 50 sec exposures gave ratios equal to 83% and 95%, respectively, whereas the ratio of the control group rose to 1837.92% after 30 days. Fig. 13 exhibits the RTV experiment results and Fig. 14 showed tumor response to therapy. The efficiency of each CAP exposure was evaluated by the log-rank test to estimate whether survival was prolonged following each exposure duration. Fig. 15 shows the survival evaluation of the three exposure durations of 20, 40, and 50 sec which indicate that treatment improved survival more than the untreated control group, but the difference is not

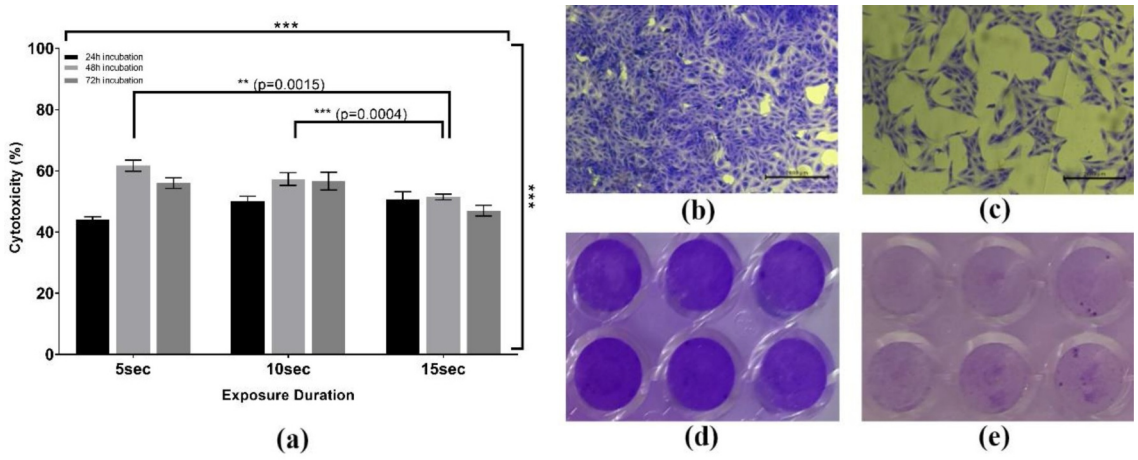

Fig. 6. CAP-treated human breast cancer MCF7 that have estrogen, progesterone receptors positive cell line, showing good response to treatment in compare to control non-treated cells. (a) Cytotoxicity assay, (b) Control cells under an inverted microscope, the images were taken at the 48h and under 10 seconds CAP exposure, crystal violet staining 10x (c) CAP-treated cells under an inverted microscope, crystal violet staining 10x, (d) control cell wells, (e) CAP-treated cell wells. Note that the stars symbols state the degree of results signification, * ($P \leq 0.05$), ** ($P \leq 0.01$), *** ($P \leq 0.001$), **** ($P \leq 0.0001$).

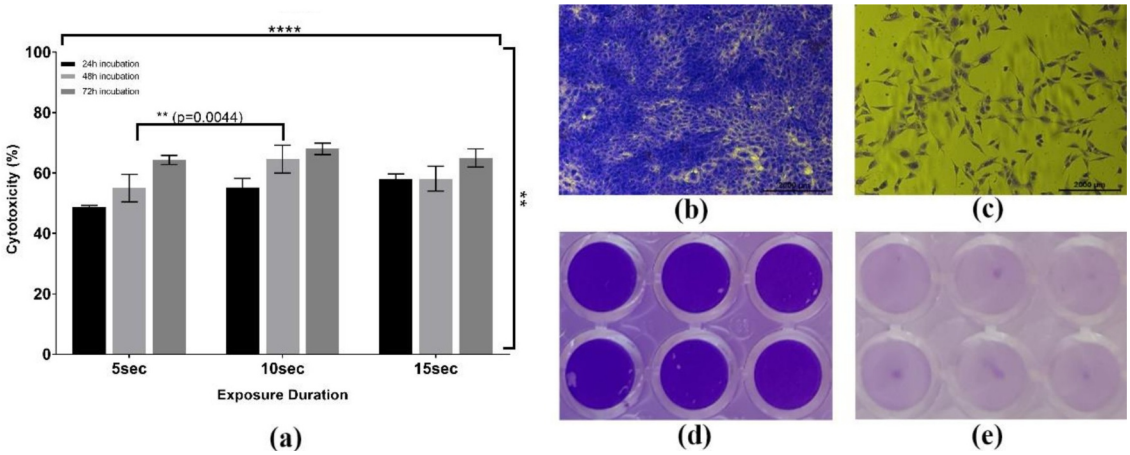

Fig. 7. CAP-treatment destroyed human breast cancer AMJ13 which is estrogen, progesterone receptors negative cell line in vitro, in compare to control non-treated cells. (a) Cytotoxicity assay, (b) control cells under an inverted microscope, the images were taken at the 48h and under 10 seconds CAP exposure, crystal violet staining 10x, (c) CAP-treated cells under an inverted microscope, crystal violet staining 10x, (d) control cell wells, (e) CAP-treated cell wells. Note that the stars symbols states the degree of results signification, * ($P \leq 0.05$), ** ($P \leq 0.01$), *** ($P \leq 0.001$), **** ($P \leq 0.0001$).

significant. Additionally, the RMW ratios were calculated using Eq. (5), which represented the mouse weights on the i^{th} day relative to those on day zero. The maximum relative weight ratio was given by the 20 sec exposure and was equal to 121.61%. The 40 and 50 sec exposures gave ratios equal to 116.55% and 106.88%, respectively, whereas the control group ratio reached 95.74% after 30 days. These results indicate that treatment improved mouse weight which is indication for mouse health unlike the control untreated mice which showed reduction in the weight due to the cachexia, Fig. 16 exhibits the RMW experiment results.

4. DISCUSSION

In the current study we tested floating-electrode DBD (FE-DBD) as source for cold plasma to be used as breast cancer therapy. In recent review by Dubuc A, et al. [22] about the use of cold-atmospheric plasma in oncology, They studied 190 original articles and reported that the most experimentally tested production system was plasma jets (72.1%) in cancer therapy research, this data may refer to the lack of enough studies about FE-DBD as cancer therapy for in vitro and vivo research. Moreover, 94.7% of these studies are in vitro, therefore our study included in vivo part, that make our study more valuable for possible clinical application in near future.

Currently, caner is a significant problem in Iraq and worldwide [23]. Breast cancer is the most threatening cancer for women with high chance for chemoresistance [24], and there is a pressing need to find a cure for this malignant disease and to overcome this chemoresistance [25]. In our study, we use cold atmospheric plasma produced by a lab-designed FE-DBD [14]. In the current work the applied voltage was 13.2KV and the frequency was 70kHz. The study showed an effect of selective cold plasma on inhibition of breast cancer cells with no effect on normal cells. Our investigation proves the strong impact of cold plasma therapy on cancerous tissue both in vitro and in vivo. Previous research has shown different possible mechanisms for the impact of cold plasma administered using a plasma jet [26, 27]. The safety and lack of harmful effect on normal cells were shown in our result at the exposure time tested, other reported safety of cold plasma in the animal model, when use plasma soft surgery that showed potential alternative treatment for ocular surface disorders to replace conventional surgery [28]. Cell viability assays showed reduction in cancer cells number with characteristic morphological changes such as nuclear condensation that described in apoptosis process [29] and some condensation of nuclear chromatin occur in necrosis as well [30]. The results of viability study and the morphological observations showed that plasma treatment

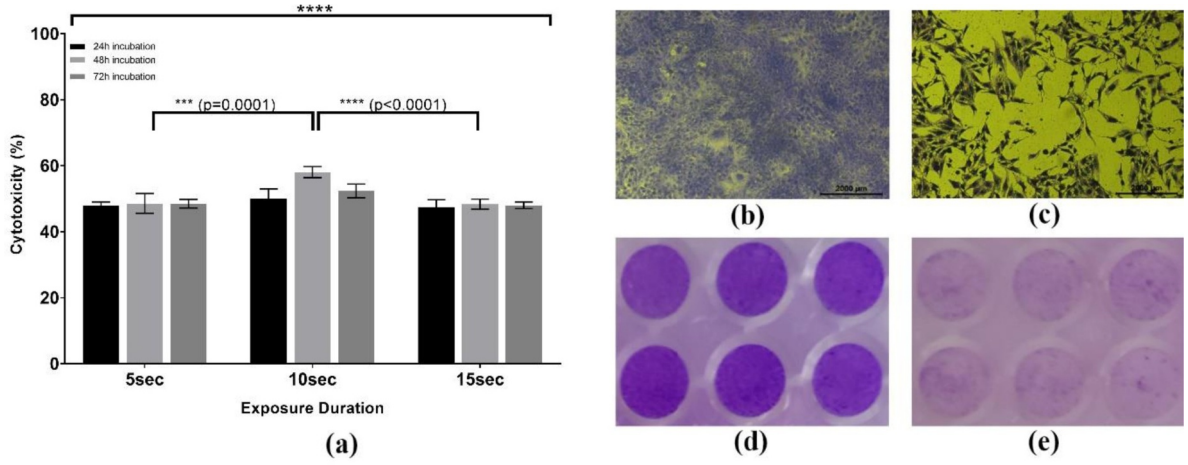

Fig. 8. CAP-treatment for mouse adenocarcinoma AMN3 cell line in vitro which is estrogen, progesterone receptors positive showed high response to treatment. (a) Cytotoxicity assay, (b) control cells under an inverted microscope, the images were taken at the 48h and under 10 seconds CAP exposure, crystal violet staining 10x, (c) CAP-treated cells under an inverted microscope, crystal violet staining 10x, (d) control cell wells, (e) CAP-treated cell wells. Note that the stars symbols states the degree of results signification, * ($P \leq 0.05$), ** ($P \leq 0.01$), *** ($P \leq 0.001$), **** ($P \leq 0.0001$).

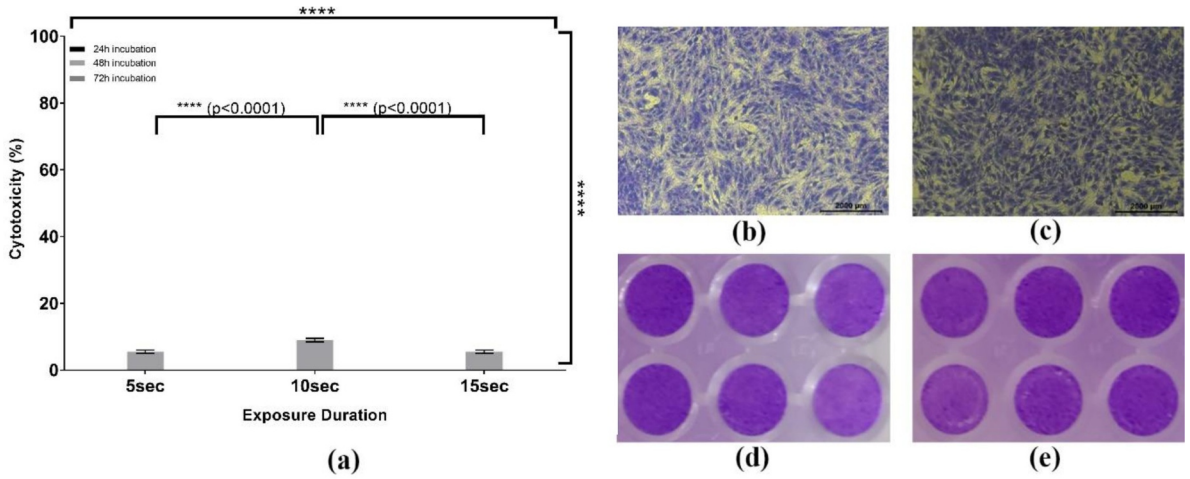

Fig. 9. Normal breast epithelial tissue HBL cell line treated with CAP in vitro. (a) Cytotoxicity, (b) control cells under an inverted microscope, the images were taken at the 48h and under 10 seconds CAP exposure, crystal violet staining 10x, (c) CAP-treated cells under an inverted microscope, crystal violet staining 10x, (d) control cell wells, (e) CAP-treated cell wells. Note that the stars symbols states the degree of results signification, * ($P \leq 0.05$), ** ($P \leq 0.01$), *** ($P \leq 0.001$), **** ($P \leq 0.0001$).

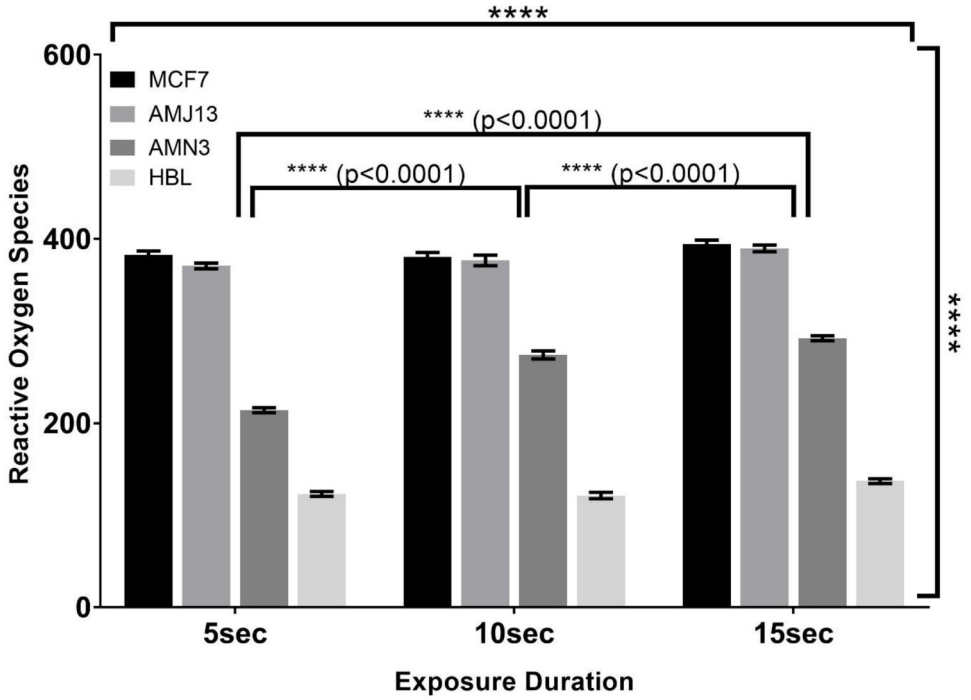

Fig. 10. ROS generated by the different cell lines in vitro. It is showing relative fluorescent intensity of treated cells to control untreated cells. Note that the stars symbols state the degree of results signification, * ($P \leq 0.05$), ** ($P \leq 0.01$), *** ($P \leq 0.001$), **** ($P \leq 0.0001$).

have high degree of selectivity as the cancer cells were detached from the plate in the plasma treated wells, while normal embryonic cells showed no detachment in the treated wells. Other researchers showing similar results for selectivity by using cold atmospheric plasma against cancer cells while showing no or mild effect against normal cells [31].

Cold plasma produces ROS, which affect apoptotic activity. The ROS generated by cold plasma mediate cold plasma-induced apoptosis and induce DNA damage [32]. Less ROS was generated by the HBL cell line after exposure to cold plasma than by the MCF7, AMN3, and AMJ13 cell lines, which indicated that the use of cold plasma increased the opportunity to impact cancerous cells and consequently induce cytotoxicity. CAP exposure can create temporal openings in the cell membrane, usually over a microsecond timescale, which allow CAP species transportation. This scenario results in different cellular responses [33]. Moreover, FE-DBD plasma induced-ROS was found to be the main antibacterial mechanism [34].

The in vitro treated cells showed different apoptosis mechanistic response under the Cap treatment, MCF7 which is estrogen, progesterone receptors positive cells showed upregulation in caspase-9 intrinsic pathway of apoptosis, while AMJ13 which is estrogen, progesterone receptors negative cells showed upregulation in caspase-8 extrinsic pathway of apoptosis and downregulation of the caspase-9 pathway with similar response in AMN3 mouse cell line. P53 was not involved in apoptosis induction as its mRNA was downregulated in all three-cell lines tested generally. Our results differ completely from another study on human colon carcinoma cells that found the activation of caspase 3 depends on the presence of p53. They report that CAP induce p53 dependent apoptosis [35]. This difference may explain by

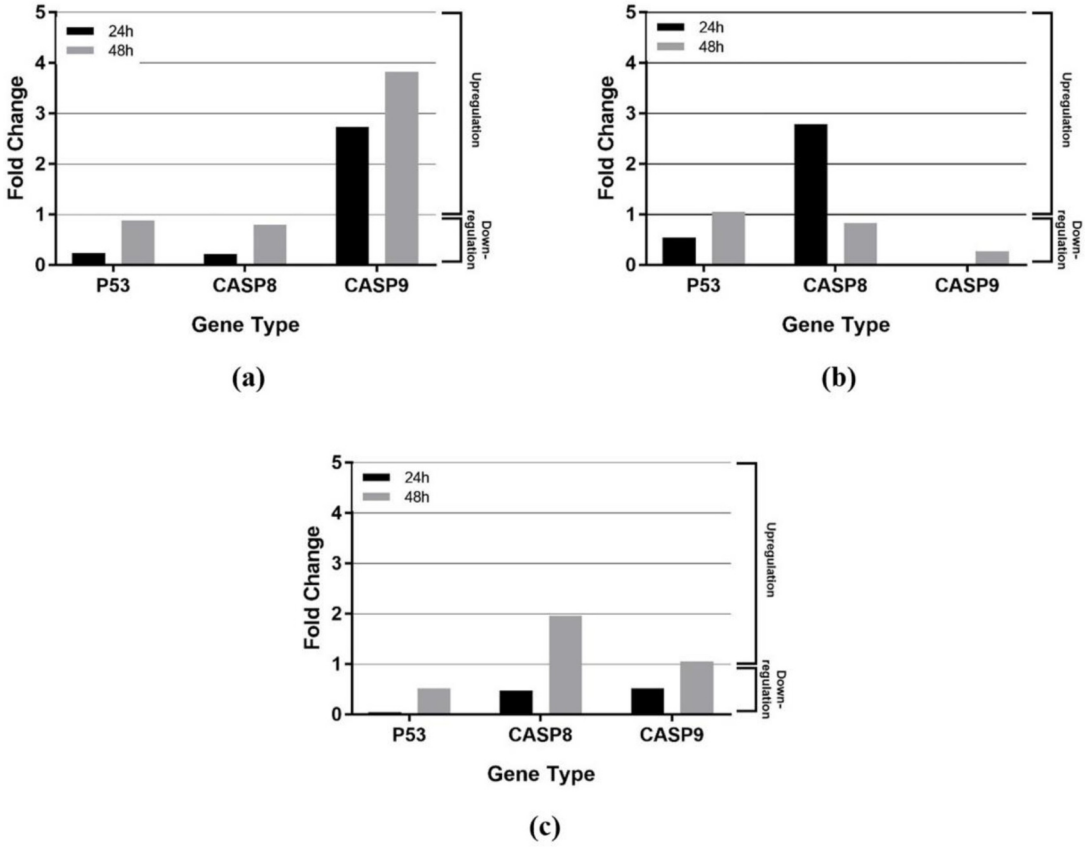

Fig. 11. Gene expression fold changes in (a) MCF7, (b) AMJ13, and (c) AMN3 cells.

Table 3
Gene expression fold change analysis

Gene	MCF7		AMJ13		AMN3	
	24 hrs	48 hrs	24 hrs	48 hrs	24 hrs	48 hrs
P53	0.2301	0.8888	0.5434	1.057	0.0448	0.5141
CASP8	0.2132	0.8011	2.7895	0.8293	0.4763	1.9588
CASP9	2.7321	3.8232	0.0001	0.2755	0.5141	1.057

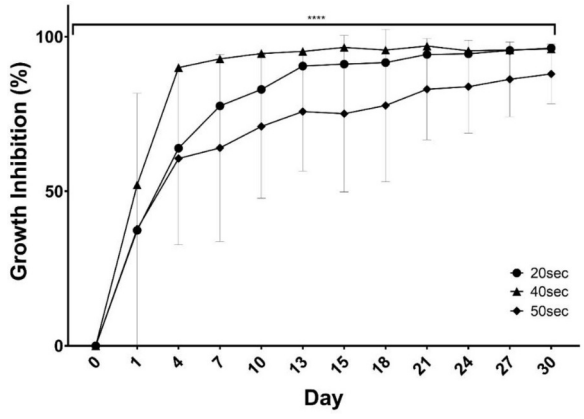

Fig. 12. Growth inhibition rates in vivo, showing the differences between the three treatment groups which indicate that 20 and 40 seconds are the most effective CAP treatment. There is significant growth inhibition with time from starting day to the end of the experiment using ANOVA 2-way test. Error bars represent standard deviation. Note that the stars symbols state the degree of results signification, * ($P \leq 0.05$), ** ($P \leq 0.01$), *** ($P \leq 0.001$), **** ($P \leq 0.0001$).

the difference in cell type and CAP source features that have been used which is non-thermal argon microwave plasma. However, Fridman et al. developed FE-DBD that induce apoptosis in melanoma skin cancer cell lines [8].

Several apoptotic and oxidative stress pathway genes were deregulated in the tumors treated with cold plasma. Moreover, the selective influence of cold plasma on several cell types suggests that the right conditions can be found to target plasma therapy to impact only cancer cells, leaving normal cells essentially unharmed. Interestingly, these results were translated to in vivo models of cancer therapy with marked reductions in tumor volumes and improved survival. Treatment with cold plasma does not result in thermal damage. Thus, development of cold plasma treatment will cause a paradigm shift in cancer therapy. Several astonishing investigations suggest that cold plasma can selectively ablate some cancer cells, such as melanoma, colon, and bladder cancer cells [26, 36, 37].

The in vivo results in the current experiment showed that 20- and 40-seconds exposure time was the best to reduce tumor volume and induced higher tumor growth inhibition to the transplanted mammary adenocarcinoma tumor. Dubuc A, et al. [22] reported presence of twenty-seven in vivo studies that concluded presence of a significant decrease in tumor size on subcutaneous tumor in mice using different type of CAP mainly jet.

Moreover, CAP tested in clinical trials on human patients with advanced head and neck cancers were treated using a plasma jet, were tumor tissue showed mild quantity of apoptotic tumor cells [38, 39].

5. Conclusions

In conclusion, the current study shows that CAP has anticancer effects both in vitro and in vivo and this effect is mediated by the ROS generated by the CAP treatment and induce apoptosis in p53

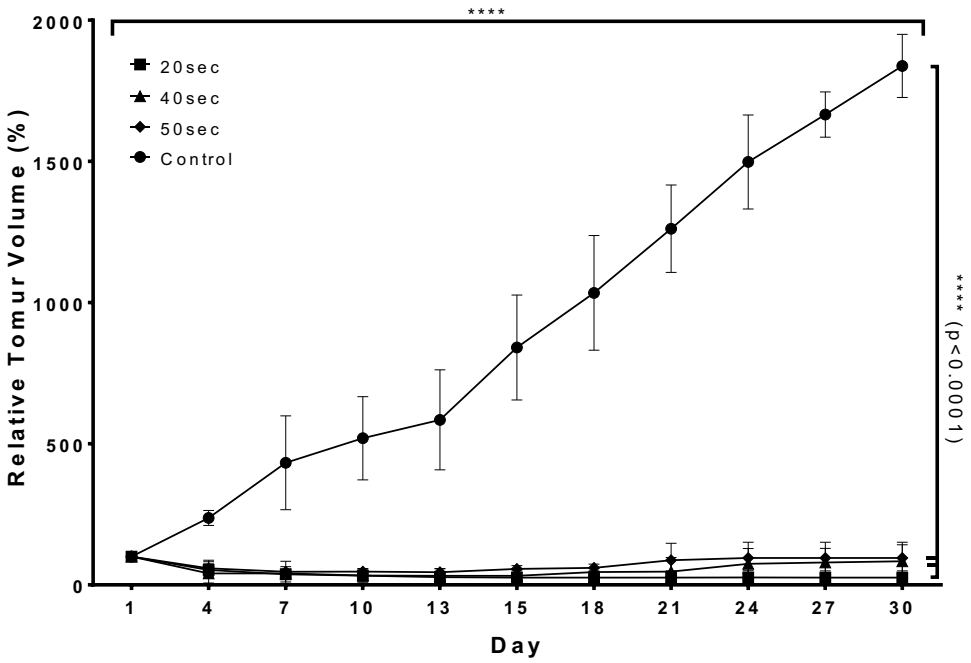

Fig. 13. Relative tumor volumes during the 30-day period, showing that CAP treatment at all exposure times induce significant tumor volume reduction in compare to non-treatment control group. Note that the stars symbols state the degree of results signification, * ($P \leq 0.05$), ** ($P \leq 0.01$), *** ($P \leq 0.001$), **** ($P \leq 0.0001$).

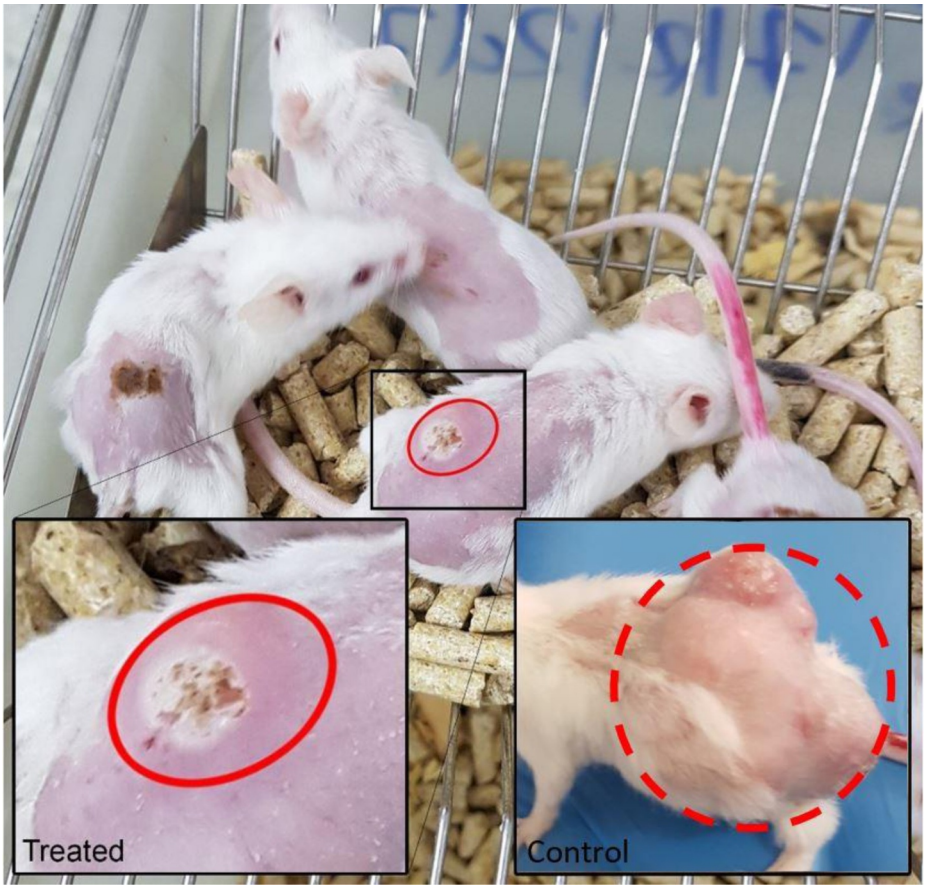

Fig. 14. The AN3 tumor-bearing mice were treated with CAP in compare to non-treated control group, and the tumor size was observed three time weekly, during the 30 days assessment period. The tumors showing in the pictures after 21 days of last dose of treatment were marked in red circles.

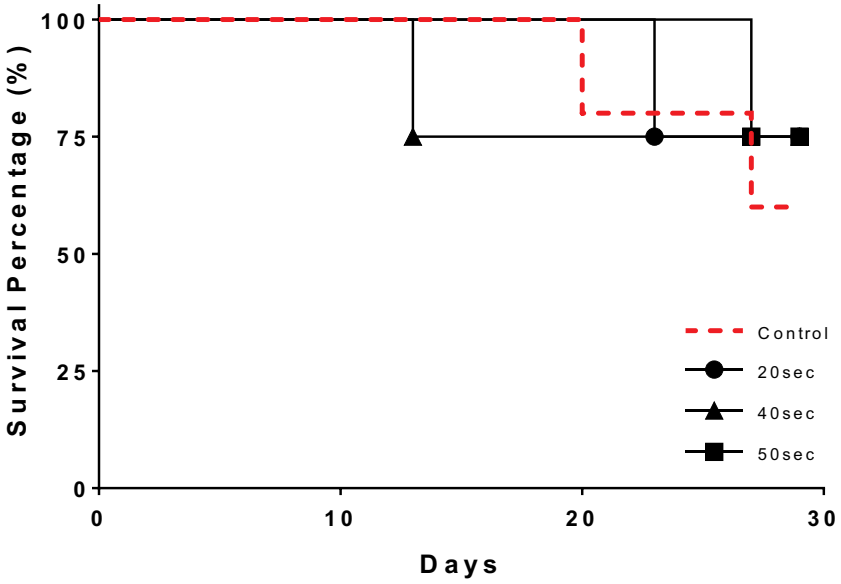

Fig. 15. Prolonged survival after different exposure durations. Survival study included treatment groups of four animals, while control group included five.

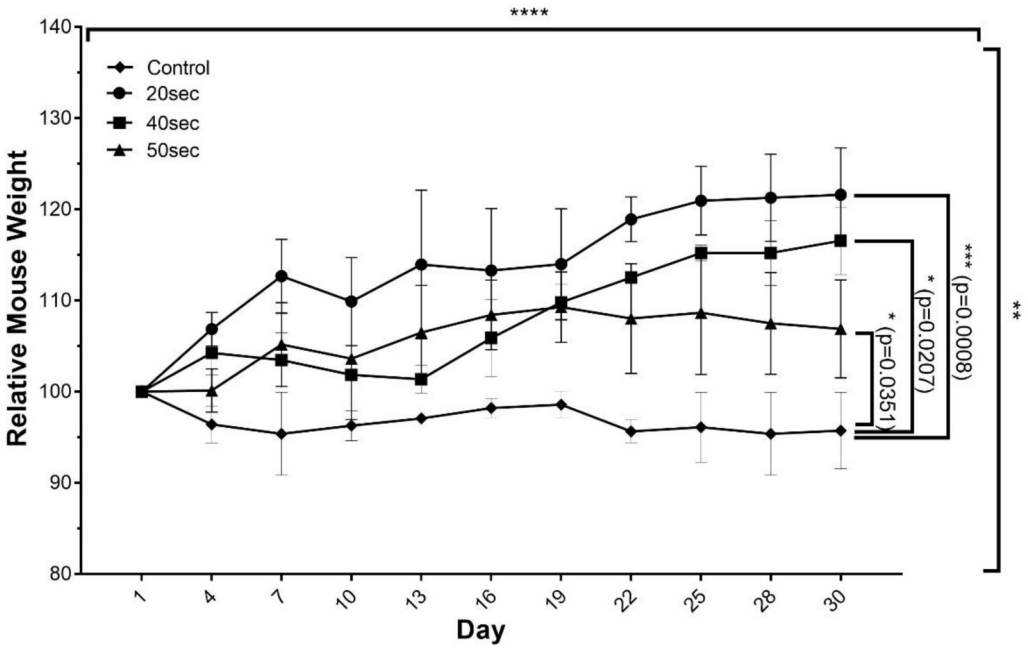

Fig. 16. Relative mouse weights during the 30-day period, showing improved mice weight in the treated groups in compare to control non treated mice, which reflect improve health of treated mice. Note that the stars symbols state the degree of results signification, * ($P \leq 0.05$), ** ($P \leq 0.01$), *** ($P \leq 0.001$), **** ($P \leq 0.0001$).

independent pathway. CAP treatment is effective and is clinically applicable for translational applications. The differences in sensitivity between different breast cancer cell lines may be related to specific differences in receptors and protein mutations. The study emphasizes that the plasma duration can affect the impact of plasma as a cancer treatment. Moreover, we found no cytotoxic effect on normal cells, suggesting promising clinical translation.

CRediT authorship contribution statement

Ban H. Adil: Methodology, Software, Data curation, Writing - original draft, Visualization, Investigation, Writing - review & editing. **Ahmed Majeed Al-Shammari:** Methodology, Software, Data curation, Writing - original draft, Visualization, Investigation, Supervision, Writing - review & editing. **Hamid H. Murbat:** Methodology, Software, Supervision.

Declaration of Competing Interest

None.

Supplementary materials

Supplementary material associated with this article can be found, in the online version, at doi:10.1016/j.cpme.2020.100103.

References

[1] F.F. Chen, Introduction to plasma physics and controlled fusion 1 Springer, 1984.
[2] A. Piel, Plasma physics: an introduction to laboratory, space, and fusion plasmas, Springer, 2017.
[3] D.B. Graves, The emerging role of reactive oxygen and nitrogen species in redox biology and some implications for plasma applications to medicine and biology, J. Phys. D Appl. Phys. 45 (26) (2012) 263001.
[4] R. Guerrero-Preston, et al., Cold atmospheric plasma treatment selectively targets head and neck squamous cell carcinoma cells, Int. J. Mol. Med. 34 (4) (2014) 941–946.
[5] M.G. Kong, et al., Plasma medicine: an introductory review, New J. Phys. 11 (11) (2009) 115012.
[6] G. Morfill, M.G. Kong, J. Zimmermann, Focus on plasma medicine, New J. Phys. 11 (11) (2009) 115011.
[7] Nehra, V., A. Kumar, and H. Dwivedi, Atmospheric non-thermal plasma sources. Int. J. Eng., 2008.2(1): p. 53-68.
[8] G. Fridman, et al., Floating electrode dielectric barrier discharge plasma in air promoting apoptotic behavior in melanoma skin cancer cell lines, Plasma Chem. Plasma Process. 27 (2) (2007) 163–176.
[9] S. Arndt, et al., Cold atmospheric plasma (CAP) changes gene expression of key molecules of the wound healing machinery and improves wound healing in vitro and in vivo, PLoS One 8 (11) (2013) e79325.
[10] C. Hoffmann, C. Berganza, J. Zhang, Cold Atmospheric Plasma: methods of production and application in dentistry and oncology, Med. Gas Res. 3 (1) (2013) 21.
[11] Brennan, S.F., et al., Dietary patterns and breast cancer risk: a systematic review and meta-analysis. 2010.91(5): p. 1294-1302.
[12] Ingvarsson, s. breast cancer: introduction. in seminars in Cancer Biol. Academic Press, 2001.
[13] A.-M. Florea, D. Büsselberg, Breast cancer and possible mechanisms of therapy resistance, J. Local and Global Health Sci. 2013 (1) (2013) 2.
[14] B.H. Adil, H.H. Murbit, A.M. Hamza, Floating Electrode dielectric barrier discharge (FE-DBD) system for biolological applications, J. Eng. Appl. Sci. 13 (SI 13) (2018) 10657–10663.
[15] Z. Ali, M. Jabir, A. Al-Shammari, Gold nanoparticles inhibiting proliferation of Human breast cancer cell line, Res. J. Biotechnol. 14 (2019) 79–82.
[16] M.A. Hamad, et al., Molecular epidemiology of bovine papillomatosis and identification of three genotypes in Central Iraq, Intervirology 60 (4) (2017) 156–164.
[17] R. Salih, et al., Antiviral effects of olea europaea leaves extract and interferon-beta on gene expression of newcastle disease virus, Adv. Anim. Vet. Sci 5 (11) (2017) 436–445.
[18] X. Rao, et al., An improvement of the 2ˆ (–delta delta CT) method for quantitative real-time polymerase chain reaction data analysis, Biostatistics, bioinformatics and biomathematics 3 (3) (2013) 71.
[19] Węglarz1½, L., et al., Quantitative analysis of the level of p53 and p21WAF1 mRNA in human colon cancer HT-29 cells treated with inositol hexaphosphate. 2006.
[20] S.H. Al-Rubae'i, T.S. Naji, K.M. Turki, Common variation of the CYP17 gene in Iraqi women with endometriosis disease, Genomics data 11 (2017) 55–59.
[21] A.M. Al-Shamery, N.Y. Yaseen, M.J. Alwan, Establishment and characterization of AN3 first murine mammary adenocarcinoma transplantable tumor line in Iraq, Iraqi J. Cancer 1 (2) (2008) 1.
[22] A. Dubuc, et al., Use of cold-atmospheric plasma in oncology: a concise systematic review, Therapeutic advances in medical oncology 10 (2018) p. 1758835918786475-1758835918786475.
[23] A.M. Al-Shammari, Environmental pollutions associated to conflicts in Iraq and related health problems, Rev. Environ. Health (2016) 245.
[24] A.M. Al-Shammari, et al., Establishment and characterization of a receptor-negative, hormone-nonresponsive breast cancer cell line from an Iraqi patient, Breast Cancer: targets and therapy 7 (2015) 223.
[25] A.M. Al-Shammari, et al., In vitro synergistic enhancement of Newcastle Disease Virus to 5-fluorouracil cytotoxicity against tumor cells, Biomed. 4 (1) (2016) 3.
[26] M. Keidar, et al., Cold atmospheric plasma in cancer therapy, Phys. Plasmas 20 (5) (2013) 057101.
[27] M. Keidar, et al., Cold plasma selectivity and the possibility of a paradigm shift in cancer therapy, Br. J. Cancer 105 (9) (2011) 1295.
[28] F. Nejat, et al., Safety evaluation of the plasma on ocular surface tissue: An animal study and histopathological findings, Clin. Plasma Med. 14 (2019) 100084.
[29] Y. Zhang, et al., Plasma membrane changes during programmed cell deaths, Cell Res. 28 (1) (2018) 9–21.
[30] L. Galluzzi, et al., Cell death modalities: classification and pathophysiological implications, Cell Death & Differentiation 14 (7) (2007) 1237–1243.
[31] M. Keidar, et al., Cold plasma selectivity and the possibility of a paradigm shift in cancer therapy, Br. J. Cancer 105 (9) (2011) 1295–1301.
[32] M. Vandamme, et al., ROS implication in a new antitumor strategy based on non-thermal plasma, Int. J. Cancer 130 (9) (2012) 2185–2194.
[33] V. Vijayarangan, et al., Cold Atmospheric Plasma Parameters Investigation for Efficient Drug Delivery in HeLa Cells, IEEE Transactions on Radiation and Plasma Medical Sci. 2 (2) (2018) 109–115.
[34] E. Kvam, et al., Nonthermal Atmospheric Plasma Rapidly Disinfects Multidrug-Resistant Microbes by Inducing Cell Surface Damage, Antimicrob. Agents Chemother. 56 (4) (2012) 2028–2036.
[35] A.I. Tuhvatulin, et al., Non-thermal Plasma Causes p53-Dependent Apoptosis in Human Colon Carcinoma Cells, Acta naturae 4 (3) (2012) 82–87.
[36] R. Reiazi, et al., Application of cold atmospheric plasma (CAP) in cancer therapy: a review, Inte. J. Cancer Manag. 10 (3) (2017).
[37] K. Nakamura, et al., A ketogenic formula prevents tumor progression and cancer cachexia by attenuating systemic inflammation in colon 26 tumor-bearing mice, Nutrients 10 (2) (2018) 206.
[38] H.-R. Metelmann, et al., Clinical experience with cold plasma in the treatment of locally advanced head and neck cancer, Clin. Plasma Med. 9 (2018) 6–13.
[39] H.-R. Metelmann, et al., Head and neck cancer treatment and physical plasma, Clin. Plasma Med. 3 (1) (2015) 17–23.